Iranian Journal of Chemical Engineering, 17 (3), 53-73, (2020) pISSN: 1735-5397
DOI: 10.22034/ijche.2021.256574.1355 eISSN: 2008-2355

Modification of Mixed Matrix Membranes' Famous Permeability Prediction Models by Considering the Formed Voids Around Nonporous Fillers

N. Sadeghi, O. Bakhtiari [*]

Membrane Research Center, Faculty of Petroleum and Chemical Engineering, Razi University, Kermanshah, Iran

ARTICLE INFO

Article history:
Received: 2020-11-09
Accepted: 2021-02-14

Keywords:
Mixed Matrix Membranes,
Permeability Prediction,
Prediction Accuracy Increment,
Maxwell Model,
Void Formation

ABSTRACT

New promising generations of mixed matrix membranes (MMMs), which potentially have better separation performances than the neat polymeric membranes, are prepared by the incorporation of proper filler particles within polymeric matrices. However, some undesired phenomena like the void formation around the filler particles limit this potential improvement. Having proper models is necessary to elucidate the impacts of this phenomenon on the MMMs' separation performance. Different models have been developed but they are not able to predict the impact(s) of formed voids truly and their predicted void permeabilities are usually overestimated. In this study, the new parameter of the modified filler volume fraction ϕ'_d considering the MMM swollen structure due to the formed voids around the filler particles, is employed along with the formed voids' permeabilities correction factor, as ß, to modify the Maxwell, Bruggeman and Pal models for the MMMs' permeability prediction. Absolute average relative errors (AAREs) of the modified models predicted that MMMs' permeabilities or selectivities were considerably reduced to 3.16, 29.92, and 21.95 % from those of the Maxwell, Bruggeman, and Pal models as 31.33, 310.64, and 67.10 % respectively. Additionally, the optimum thicknesses of the formed voids around the filler particles rationally agree with the Knudsen flow concepts.

1. Introduction

The gas separation is widely employed in different industrial processes e.g. the natural gas sweetening, recovery of landfill gas, air separation, separation of olefin/paraffin, and recovery of hydrogen [1-3]. Different processes such as the chemical and physical absorptions, cryogenic distillation, adsorption, and membrane separation are developed and employed for these purposes [4]. Among them membrane processes are more attractive due to their ease of scaling-up and operation, high process flexibility, efficient energy consumption, environmental friendlyness, and continuous improvement of the current membrane material(s) and/or introduction of new membrane materials, as the most important superior advantage over the other processes [5-7]. Polymers, due to their processability into the large surface area

[*]Corresponding author: obakhtiari@razi.ac.ir (O. Bakhtiari)

required for the industrial application, proper mechanical and thermal stability, low cost, ease of operation, acceptable separation performance, high energy efficiency and generally speaking tailor-made properties, are dominant materials among different materials used for the membranes preparation [8-10]. However, the polymeric membranes separation performance is limited by a trade-off between permeability and selectivity as presented by Robeson [11-14] which states that the increase in membrane selectivity is compensated by lowering its permeability and vice versa. Swelling phenomena in the polymeric membrane, especially in the presence of condensable molecules, is another problem which leads to losing the membrane separation performance [15, 16]. Therefore, many efforts, like crosslinking [17-19], blending [18], grafting [20, 21], and even though simultaneous modifications [22], have been made to enhance the polymeric membranes separation performance.

Mixed matrix membranes (MMMs), as the new generation of the membranes, are considered as candidates to overcome the shortcomings of polymeric membranes and are promising to improve the position of the current membrane processes in different industries [23-26]. Generally speaking, proper inorganic filler particles are incorporated into proper polymer matrices as the dispersed phase to prepare MMMs with higher potential separation performances and maybe antibacterial, fouling resistance, thermal and mechanical properties [27-29].

The gas permeability through the MMMs depends on many factors such as their filler particles and the polymer's properties, the interface of their filler-polymer matrix, the filler particles agglomeration (if any), the inorganic filler type and the filler particles loadings [4, 25, 30]. Different types of filler particles, such as carbon molecular sieves, zeolites, metal organic frameworks, mesoporous and microporous molecular sieves, metal oxides nanoparticles, clays and silica [30-33], are used as MMMs' dispersed phase.

In an ideal MMM structure, polymeric chains come into intimate contact with the filler particles surface with the clearly distinguishable interface. However, in many real MMMs structures, some non-ideal morphologies (defects), such as the filler particles pore blockage, polymer chains' rigidification and/or interface void formation, may occur during the MMMs' preparation due to the different properties of the (inorganic) filler particles and polymer matrices [33-35]. Each case has its own impact on the MMMs performance, e.g. interfacial voids result in the increment of MMMs' permeabilities and the decrement of selectivities. Knowing different impact(s) of above cases on the MMMs' separation performance helps to design better MMMs' structures and achieve higher separation performances [33, 34]. Also due to the different nature and mass transfer mechanism of the comprised phases of filler particles and polymers in MMMs, i.e. the Knudsen flow, solution diffusion, surface flow, etc., penetrants have different tendencies toward them and should be considered in the MMMs constructing materials and possible emerging interphases layers [1, 31, 36].

Some researches were also carried out on the MMMs' permeability prediction using analytical models [28, 37] and some proper simulation software for computational fluid dynamics (CFD) [38]. On the other hand, some different models, such as the Maxwell (1873), the Bruggeman (1935), the Pal, the

Lewis-Nielson and the Fleske [39], were developed for the MMMs' separation performance prediction. These models are reviewed at first and then a new improved model is presented to predict the MMMs' separation performance in case of the void formation.

2. Some MMMs' separation performance prediction models

The currunt predicting models for MMMs' separation performance have been originally developed to predict the composite materials' thermal/electrical conduction and are used according to the thermal/electrical conduction analogies and the gaseous penetrants permeation through MMMs [40]. The Maxwell model was employed for the MMMs' permeabilities prediction in 1997 as per the following equation [41-43]:

$$P_r = \frac{P_{MMM}}{P_c} = \frac{P_d + 2P_c - 2\phi_d(P_c - P_d)}{P_d + 2P_c + \phi_d(P_c - P_d)} \quad (1)$$

where P_r is the permeability ratio, P_{MMM}/P_c, P_{MMM}, P_c and P_d are permeabilities of MMM, polymer (continuous phase) and filler particles (dispersed phase) respectively and ϕ_d is the volume fraction of the dispersed phase. Although the Maxwell model is an easy explicit equation for predicting the MMMs' permeability, it ignores the effects of the filler particle size distribution, shape, and aggregation. Moreover, the Maxwell model is not valid for filler volume fractions higher than 20-25 Vol. % [34, 42].

The Bruggeman model was adapted for the MMMs' permeability prediction over a wide range of filler particles loading and expressed as per the following equation [42]:

$$\frac{(P_{MMM}/P_c) - (P_d/P_c)}{1 - (P_d/P_c)}\left(\frac{P_{MMM}}{P_c}\right)^{-1/3} = 1 - \phi_d \quad (2)$$

Like the Maxwell model, the effects of the filler particles' shape, size distribution, and aggregation are not also considered in the Bruggeman model. The Bruggeman model is an implicit equation that should be solved numerically for P_{MMM} by an appropriate method such as the Newton-Raphson or fixed point method [34, 42, 44, 45].

The Pal model was applied for predicting the MMMs' permeability which can be calculated using the following equation [36, 42]:

$$\left(\frac{(P_d/P_c) - 1}{(P_d/P_c) - (P_{MMM}/P_c)}\right)\left(\frac{P_{MMM}}{P_c}\right)^{1/3} = \left(1 - \frac{\phi}{\phi_m}\right)^{-\phi_m} \quad (3)$$

where ϕ_m is the maximum filler particles' volume fraction in the MMMs assumed as the random close packed spheres and considered as 0.64. It is worth noting that, as ϕ_m approaches to unit ($\phi_m \rightarrow 1$), this model reduces to the Bruggeman model. Since ϕ_m is a function of particles size distribution, particle shape, and aggregation (if any), effect of the MMM morphology is considered by the Pal model. Similar to the Bruggeman model, this model has an implicit equation and needs to be solved numerically [33, 34].

There are many other models available for the prediction of gas permeation through

MMMs that can be found elsewhere [16, 33, 34, 46, 47]. Among them, the Maxwell, the Bruggeman and the Pal models are the most famous and selected for further analysis and comparison in the current study [33]. As it was mentioned above, in the case of voids formation around the filler particles, there are many phenomena occur which have considerable impacts on their containing MMMs separation performance. In this study, two parameters are introduced to the selected predictive models in order to take into account the two main phenomena of swollen MMMs due to formed voids (via ϕ'_d parameter) and overestimated Knudsen model predicted permeabilities (via β parameter). The impacts of theses parameters on the accuracy of the models prediction will be discussed in the following sections.

3. Models and methods

3.1. MMMs' permeability prediction models used for the formed voids around the filler particles

The formed voids around the incorporated filler particles into the MMMs' structure can be considered as a third phase and its permeability may be calculated by using the Knudsen flow. As the voids have formed around the filler paratciels, it is assumed that there is no intimate contact between them and the polymer chains in the third phases, i.e. the third phase makes a clear distance between filler particles and polymer chains. The gas permeability of formed voids, P_I, is considered as the product of the modified Knudsen diffusion, D, and molecular solubility (concentration), S, in formed voids which can be calculated using the following equation [10]:

$$P_I = DS \tag{4}$$

$$D = D_{Knudsen}\left(1 - \frac{\sigma_p}{2l_I}\right) \tag{5}$$

$$D_{Knudsen} = (d_{Pore}/3)(8RT/\pi M_I)^{1/2} \tag{6}$$

$$S = \frac{1}{RT}\left(1 - \frac{\sigma_p}{2l_I}\right)^2 \tag{7}$$

where σ_p is the Lennard-Jones diameter of the gaseous penetrant as reported in Table 1, l_I is the effective thickness of the formed void around the filler particles, d_{Pore} is the pore diameter which is approximating to $2\,l_I$, R is the universal gas constant, T is the absolute temperature, and M_I is the molecular weight of the penetrant. It should be noted that, in case of employing the Knudsen flow concept, the micro-volume of the formed void is assumed to be the same as that of the macro-void and the solubility is calculated based on this assumption [48, 49].

Table 1
Molecular properties of gaseous penetrants [52].

Gas molecule	Kinetic diameter, d_k (Å)	Lennard-Jones diameter, d_{LJ} (Å)
He	2.6	2.55
H_2	2.89	2.83
O_2	3.46	3.47
N_2	3.64	3.8
CO_2	3.3	3.94
CH_4	3.8	3.76

Thereafter, the "effective filler particles permeability, P_{eff}," is calculated by applying a proper MMMs' permeability prediction model such as the Maxwell model and considering filler particles as incorporated into a pseudo-continuous phase of the formed voids [16]:

$$P_{eff} = P_I \left[\frac{P_d + 2P_I - 2\phi_s(P_I - P_d)}{P_d + 2P_I + \phi_s(P_I - P_d)}\right] \quad (8)$$

$$\phi_s = \frac{\phi_d}{\phi_d + \phi_I} = \left(\frac{r_d}{r_d + l_I}\right)^3 \quad (9)$$

where ϕ_s is the volume fraction of the filler particles in the formed voids, r_d is the average filler particles' radius and ϕ_I is the volume fraction of the formed voids in the total MMM volume.

After the P_{eff} estimation, the selected predictive model of Maxwell is applied again to calculate the MMM permeability according to the following equations [33, 46, 50]:

$$\phi_s = \frac{\phi_d}{\phi_d + \phi_I} = \left(\frac{r_d}{r_d + l_I}\right)^3 \quad (10)$$

$$P_{MMM} = P_c \left[\frac{P_{eff} + 2P_c - 2(\phi_d + \phi_I)(P_c - P_{eff})}{P_{eff} + 2P_c + (\phi_d + \phi_I)(P_c - P_{eff})}\right] \quad (11)$$

This two step Maxwell model is shown schematically in Figure 1. Also, this approach can be used for other models such as Bruggeman and Pal models.

The estimated voids permeabilities, P_I, by the first step of this approach, seem to be overestimated, as being calculated and demonstrated in Figure S 1, which are up to 6 orders of magnitude (10^6) and much higher than those reported by Shelekhin et al. (Figure 2) [51].

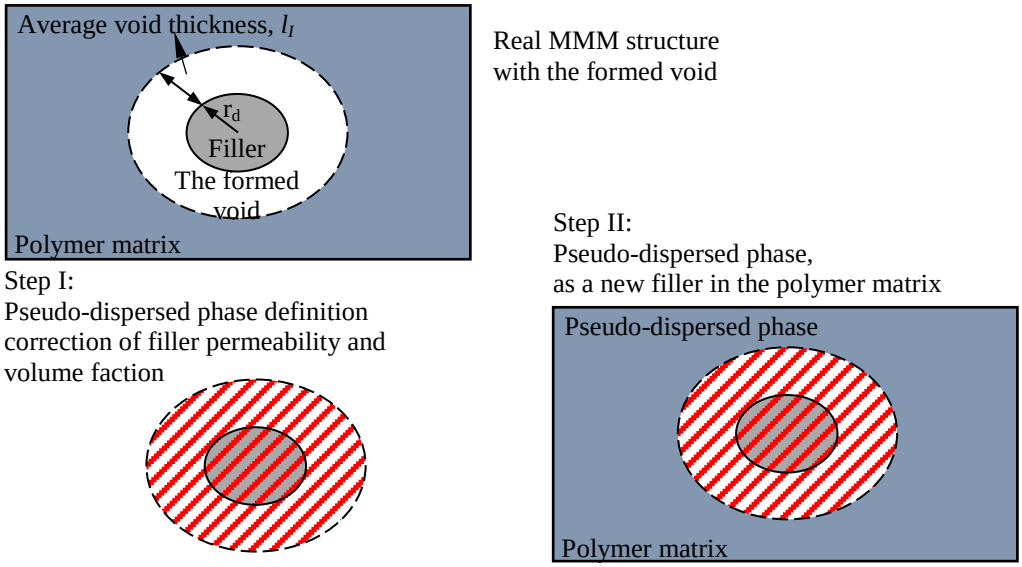

Figure 1. Schematic representation of the two step Maxwell model for the permeability prediction of a real MMM with the formed voids around the filler particles.

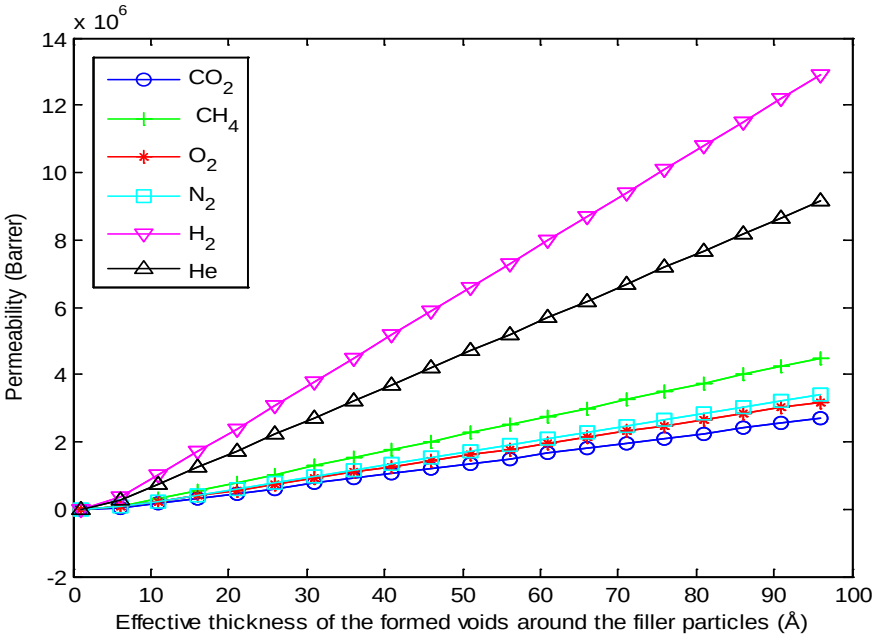

Figure S 1. Calculated permeabilities of different gaseous penetrants through the formed voids around filler particles vs. the effective void thickness based on the Knudsen flow concept [55].

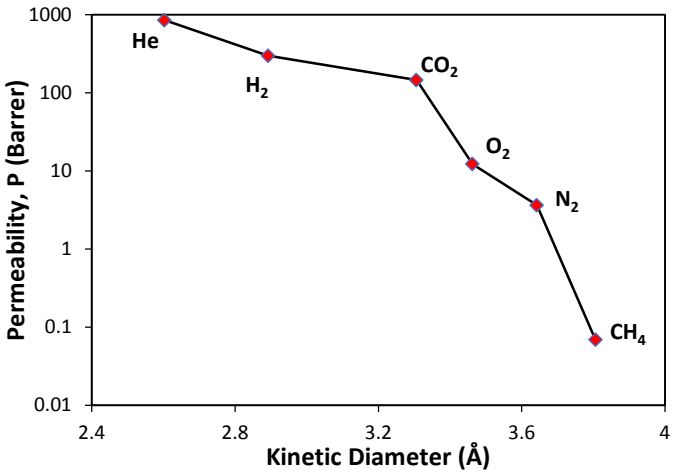

Figure 2. Permeability of different gaseous penetrants through fine silica hollow fibers with an average pore size of 20 μm, as reported by Shelekhin et al. [51].

The maximum void permeability value reported by Shelekhin et al. is around 1000 Barrers for He through 20 μm pores. It should be noted that the average pore size reported by Shelekhin et al. was 20 μm which was around 10^4 times greater than the voids thickness (Å) formed in MMMs, so their permeability should be higher than the MMMs' voids permeability. But, as it can be observed in Figure S 1 and Figure 2 voids permeabilities calculated by Eq. (4) are much higher than those reported by Shelekhin et al. Consequently, it was decided in the current study to correct those permeabilities by their multiplication by the void permeability adjustment parameter, β. Besides considering the first parameter of l_I, the modified models become higher accurate after the introducion of the second parameter of β.

$$P_I = 0.53 \times \beta \times \left(d_{Pore}/\sqrt{M_I RT}\right) \times \left(1 - \sigma_p/2l_I\right)^3 \quad (12)$$

It should be noted that many other research works have been done in the area of the prediction of MMMs' permeabilities with the voids around the filler particles but none of them report the optimized value(s) of l_I [9, 42, 48]. In the following section, the l_I values obtained by the Maxwell, the Bruggeman, the Pal, and the Modified Models will be reported and also the impact of the β parameter introduction on l_I and the prediction accuracy will be discussed.

On the other hand, considering the void formation around the filler particles, the volume fraction of the pseudo-two phase filler particles was corrected by the introduction of the new parameter of ϕ'_d instead of its previous proposed value of $\phi_d + \phi_I$ [28] in Eq. 13, which is defined by the following equation:

$$\phi'_d = \frac{\phi_d/\phi_s}{1 - \phi_d + \phi'_d} \quad (13)$$

The parameter of ϕ'_d is introduced since the MMMs' body is swollen after the void formation around the filler particles and then the volume fraction is recalculated accordingly. If the total volume of MMM was considered to be as the unit volume, the modified volume of the swollen membrane would be $1 - \phi_d + \phi'_d$ which was the sum of the volumes of the polymer, the filler particles and the formed voids. On the other hand, ϕ_d/ϕ_s is the volume ratio of the filler and the formed voids.

In the two step approach, the selected predictive model(s) is used to combine permeabilities of the filler particles, the formed voids around the filler particles and the polymer matrix to predict MMMs' permeability [10].

3.2. MMMs' Permeability Prediction and their Error Calculation

Generally, the only variable that can influence the MMMs' permeability in this method is l_I and its optimum value is determined by the least square method, e.g. minimum S in the following equation:

$$S = \sum_{i=1}^{N} \left(P_i^{cal} - P_i^{exp}\right)^2 \quad (14)$$

where P_i^{cal} and P_i^{exp} are the calculated and experimentally measured MMMs' permeabilities at a certain filler particles loading and N is the number of experimental data points.

In the modified predictive model(s) in the current study, the β parameter is used for the permeability correction of the formed voids around filler particles incorporated into MMMs and then the corrected permeability is used for the two step prediction approach. In this way, the second parameter of β and that of l_I enable the modified model to fit much better the experimental measured data. The optimum values of l_I and β are determined by the least square method, also.

After the calculation of MMMs' permeabilities at different values of l_I and/or β, the absolute average relative error percentage (AARE) is calculated by the following equation [33]:

$$\text{AARE}\ (\%) = \frac{100}{N}\sum_{i=1}^{N}\left|\frac{P_i^{cal} - P_i^{exp}}{P_i^{exp}}\right| \quad (15)$$

where N is the number of experimental data points. In the following section, different MMMs' permeabilities, which are predicted using both current and modified models, will be discussed. All the calculations were done using some Matlab codes developed in Matlab 2014b software.

4. Results and discussion

Some data of the experimentally measured permeabilities of different MMMs with formed voids around the incorporated filler particles were gathered from relevant published papers and reported in Table S 1. After that, the existing predictive model developed for MMMs' permeabilities and the current proposed modified model have been employed to predict the experimentally measured MMMs' permeabilities. Optimum values of the model's parameter(s) are obtained by the least square method and AAREs are calculated and discussed in the following section.

Table S 1
Experimentally measured permeabilities of different MMMs published in the related literature.

Membrane	Filler loading (Vol. fraction)	Permeability (Barrer)						MMMs ideal selectivity					Temp. (K)	Ref.
		P_{CO_2}	P_{CH_4}	P_{H_2}	P_{O_2}	P_{N_2}	P_{He}	S_{H_2/CH_4}	S_{He/N_2}	S_{CO_2/CH_4}	S_{O_2/N_2}	S_{He/CH_4}		
Polysulfone-fumed silica (TS530)	0		0.22	11.8		0.24	11.8	53.64	49.16				308	[52]
	0.05		0.29	13.8		0.31	13.1	47.58	42.26					
	0.10		0.38	15.9		0.4	14.9	41.84	37.25					
	0.15		0.62	22.7		0.67	20.1	36.61	30					
	0.20		1.1	32.3		1.12	27.7	29.36	24.37					
PCPA-fumed silica (TS530)	0		2.8	49	8.6	1.8	33	17.5	18.33		4.77	11.785	298	[56]
	0.058		5.6	110	18	4	67	19.64	16.75		4.5	11.964		
	0.19		53	350	86	28	220	6.6	7.86		3.07	4.151		
Matrimid-TiO_2	0	4.3	0.21		1.29	0.22	8.75		39.77	20.48	5.86		308	[57]
	0.05	5.4	0.32		1.6	0.36	11.2		31.11	16.87	4.44			
	0.10	7.4	0.41		1.75	0.5	13.4		26.8	18.05	3.5			
	0.15	8	0.58		1.86	0.74	15.2		20.54	13.79	2.51			
	0.20	10.54	0.77		2.45	0.92	19		20.65	13.69	2.66			
	0.25	12	1.84		3.25	1.35	25.2		18.66	6.52	2.41			
ULTEM-fumed silica (TS610)	0		0.04		0.34	0.05	6.95				6.8	173.75	308	[54]
	0.06		0.043		0.36	0.06	7.02				6	163.25		

	0.11		0.064	0.58	0.1	10.08		5.8	157.5		
	0.18		0.087	0.6	0.12	8.3		5	95.4		
ULTEM-fumed silica (TS530, melt processed)	0	1.36	0.04				34.00			308	[54]
	0.01	1.3	0.05				27.68				
	0.07	2.51	0.11				22.38				
	0.10	2.88	0.12				26.17				
ULTEM-fumed silica (TS530, solution casted)	0		0.04			6.95			173.75	308	[54]
	0.07		0.158			14.456			91.49		
	0.13		0.367			15.91			43.35		
	0.20		0.71			23.49			33.08		
ULTEM-fumed silica (TS720, melt processed)	0		0.04	0.43	0.08	9.06		5.37	226.5	308	[54]
	0.02		0.05	0.48	0.12	10.08		4.00	201.6		
	0.04		0.08	0.69	0.14	12.42		4.93	155.25		
	0.10		0.09	0.73	0.18	10.54		4.33	117.11		
ULTEM-untreated SiO_2	0		0.04			6.95			173.75	308	[54]
	0.04		0.05			8.21			152.11		
	0.06		0.07			8.77			120.15		
	0.08		0.07			11.72			169.18		
	0.10		0.08			12.79			162.78		

Table 2 demonstrates the comparison between predicting abilities of the three available models of the Maxwell, the Bruggeman and the Pal, and their modified ones for O_2, N_2, and He permeabilities and O_2/N_2 and He/N_2 selectivities through poly (1-chloro-2-phenylacetylene) (PCPA)-Fumed Silica (FS) MMM at 25 °C. As it can be observed, AAREs of both permeabilities and selectivities reduced after the introduction of β and the correction of the filler particles loadings, ϕ'_d, except for those of the Bruggeman model. AARE for selectivities become much less in compared with the original models. Surprisingly, the AARE of O_2/N_2 selectivity using the Bruggeman model is 24.31 % and after employing β and ϕ'_d it becomes equal to 60.53. However, it is worthy to note that the thickness of the formed void layer surrounding the nanoparticle, l_I, is calculated as 2.2 Å at the beginning which is smaller than the diameter of the penetrating molecules. The experimental data for this system implies an increment in the O_2 and N_2 permeabilities and a reduction in their selectivity which means some voids are formed around the filler particles. Therefore, l_I value should be larger

than the penetrate's diameter and its value was logical as the model was modified by introducing β and ϕ'_d parameters, i. e. l_I was calculated as 80.2 Å.

The comparisons between the predictions accuracy (e.g., AARE) for the studied models for different experimental data is reported in Table 3. For polysulfone-silica MMM, the AAREs of N_2 permeabilities and selectivities for the Bruggeman model are larger than 100 % while after the introduction of β and ϕ'_d parameters they are reduced to some acceptable values as well as those for the Matrimid-TiO_2 selectivity. As it is shown in Table 3, the formed voids' optimized thicknesses, l_I, are logical and the calculated AAREs for both permeabilities and selectivities are reduced indicating the effectiveness of the β parameter introduction and the ϕ'_d correction.

Table 2
Comparison between the AAREs of original and modified models' prediction for the experimental data [56] of O_2, N_2, and He Permeation and O_2/N_2 and He/N_2 selectivities of PCPA-fumed silica (FS) MMMs at 25 °C.

Predictive model	l_I (Å)	β	AARE (%)			l_I (Å)	β	AARE (%)		
			P_{O_2}	P_{N_2}	α_{O_2/N_2}			P_{He}	P_{N_2}	α_{He/N_2}
The Maxwell	18.9	-	10.51	14.44	15.77	32.7	-	7.18	39.07	71.38
The Modified Maxwell	61.9	0.00012	4.22	3.96	0.89	62	0.000071	0.85	3.72	0.97
The Bruggeman	2.2	-	68.35	71.20	24.31	1.87	-	62.336	77.348	197.1
The Modified Bruggeman	80.2	0.000009	49.56	10.96	60.53	43.5	0.00001	42.52	11.01	31.83
The Pal	1.8	-	78.01	70.21	95.87	27.3	-	17.14	48.34	71.38
The Modified Pal	58.1	0.00001	56.33	14.54	52.92	31.3	0.00029	16.97	30.53	21.26

Table 3
Prediction of different MMMs' selectivities and permeabilities with the formed voids around the filler particles.

MMM	Predictive model	l_I (Å)	β	AARE (%)		
				P_{He}	P_{N_2}	α_{He/N_2}
Polysulfone-Silica [52]	The Maxwell	10.2	-	11.88	22.88	52.74
	The Modified Maxwell	31.1	0.000028	5.25	11.17	2.08
	The Bruggeman	1.7	-	46.87	143.05	905.2
	The Modified Bruggeman	14.5	0.00001	23.54	35.34	7.48
	The Pal	15.3	-	4.62	28.22	52.75
	The Modified Pal	28.2	0.000051	4.56	13.48	25.12
MMM	**Predictive Model**	**l_I (Å)**	**β**	**P_{O_2}**	**P_{N_2}**	**α_{O_2/N_2}**
Matrimid-TiO_2 [57]	The Maxwell	2.1	-	10.16	42.59	99.23
	The Modified Maxwell	10.5	0.000023	7.35	2.84	10.09
	The Bruggeman	1.9	-	55.82	73.22	387.17
	The Modified Bruggeman	13.1	0.0000061	34.01	4.26	34.48
	The Pal	3.4	-	6.63	43.17	75.01
	The Modified Pal	9.3	0.00001	6.50	4.06	41.25
MMM	**Predictive Model**	**l_I (Å)**	**β**	**P_{CO_2}**	**P_{CH_4}**	**α_{CO_2/CH_4}**
ULTEM-fumed silica (TS530, melt	The Maxwell	56.7	-	8.99	21.97	40.50
	The Modified Maxwell	83.8	0.00001	7.90	12.35	23.40

processed) [54]	The Bruggeman	1.9	-	38.33	53.39	39.44
	The Modified Bruggeman	6.2	0.00003	38.15	45.98	15.26
	The Pal	1.9	-	34.20	84.10	40.49
	The Modified Pal	20	0.00002	33.98	41.29	19.21

Figure 3 presents a comparison between the prediction abilities of three current predictive models and their modified ones for the CO_2 and CH_4 permeabilities and CO_2/CH_4 selectivities through ULTEM-Fumed Silica (TS530, melt processed) MMMs.

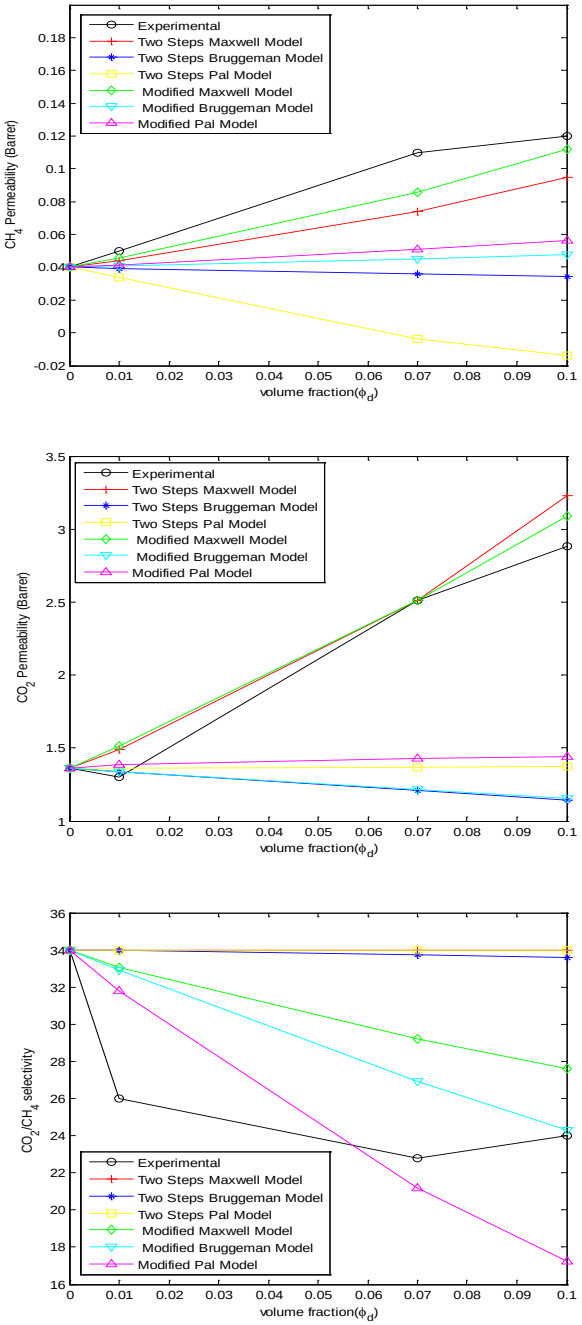

Figure 3. Comparison between the experimental [54] and predicted CO_2 and CH_4 permeabilities and selectivities through ULTEM-fumed silica (TS530, melt processed) MMMs using different original predictive models and their modified models.

As it is shown in these systems, Maxwell and Modified Maxwell models have good accuracy, so in the following Maxwell and Modified Maxwell model will be investigated.

Juhyeon et al. prepared some MMMs by the incorporation of silica nanoparticles into polysulfone polymer matrix, and showed the formed voids around the filler particles [52]. The optimum value of l_I, having employed the two step Maxwell model to predict these MMMs' permeabilities, was obtained and acceptable AAREs, for H_2 and CH_4, were calculated as reported in Table 4. However, the calculated ideal MMMs' selectivities remain nearly equal to that of the neat polymeric membrane, and independent of filler particles loadings. This is due to the fact that the estimated permeabilities of the formed voids are overestimated (Figure S 1) in the entire investigated l_I range of 1-80 Å.

Table 4
Comparison of the ideal and the modified Maxwell models' AAREs for permeabilities' prediction of the experimentally measured data of H_2 and CH_4 through polysulfone-silica MMMs [52].

Predictive model	l_I (Å)	β	AARE (%)		
			P_{H_2}	P_{CH_4}	α_{H_2/CH_4}
The Maxwell	14.6	-	11.79	18.34	42.52
The Modified Maxwell	30.7	0.00003	11.34	14.72	3.90

After the correction of the void permeabilities by the introduction of the β parameter and the formed voids volume fraction by the parameter of ϕ'_d, the fitness of both permeability and selectivity curves considerably improved. It can be confirmed by very smaller calculated AAREs of H_2/CH_4 selectivities and permeabilities of H_2 and CH_4, Table 4. On the other hand, the Knudsen flow is the dominant flow regime in the pores having diameters in the range of 20-1000 Å [53]. As it can be understood from Table 4, the optimum value of l_I for the two step Maxwell model is not in this range while that of the current modified model is. For H_2 and CH_4 permeabilities, the modified current model showed relatively lower AAREs of 11.34 and 14.72 % respectively, compared with the two step Maxwell model (AAREs of 11.79 and 18.34 %, respectively). While the optimum value of the β parameter is very small and it lowers the formed voids' permeabilities by several orders of magnitude, but the volume fraction of the formed voids in the MMMs' structure is not high enough to change the MMMs' effective permeability considerably. The main improvement of the modified current model is in the higher accuracy of H_2/CH_4 selectivities' prediction as 3.90 % for AAREs compared with that of 42.52 % for the two step Maxwell model. This can be attributed to the fact that the formed voids permeabilities in the Knudsen mechanism are higher than actual values.

The graphical comparison between both the existing two step and modified predictive models are presented in Figure 4 for the permeabilities of H_2 and CH_4 and H_2/CH_4 selectivities in polysulfone-silica MMMs [52]. The current modified Maxwell model obviously has a higher prediction accuracy than that of the two step Maxwell model, especially for MMMs' selectivities' prediction. This can be attributed to the fact that the permeabilities of the formed voids around the filler particles have became closer to their actual values.

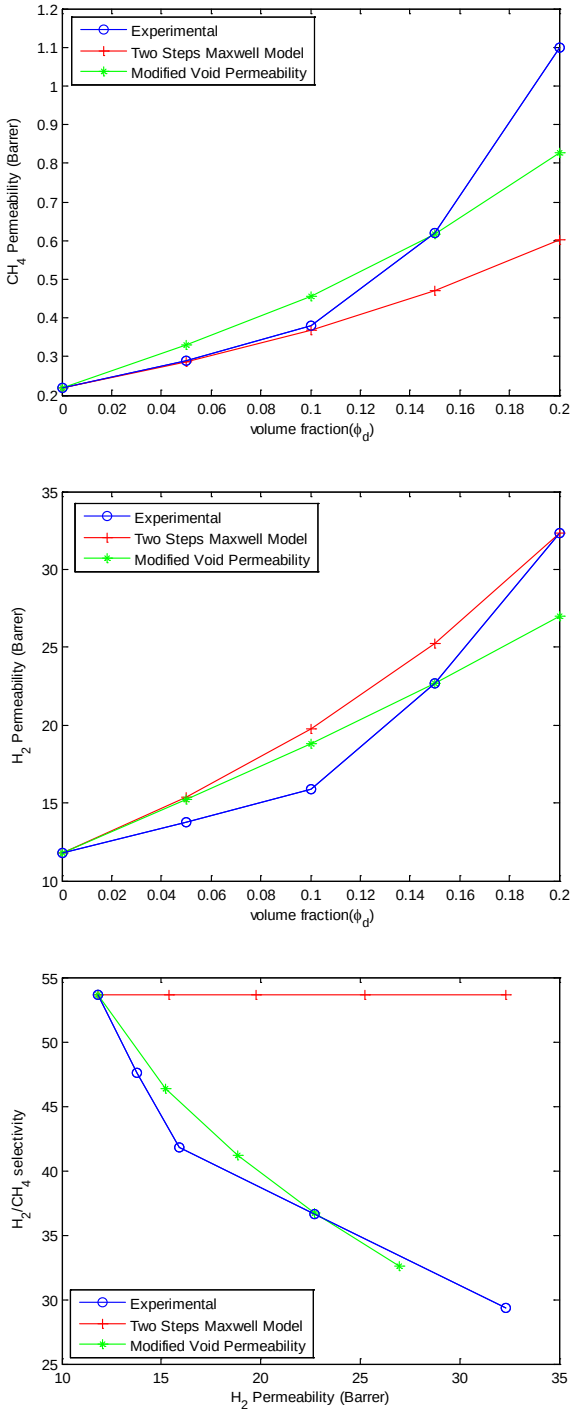

Figure 3. Comparison between the experimental H_2 and CH_4 permeabilities and H_2/CH_4 ideal selectivities through the polysulfone-silica MMMs [52] and those predicted using the current modified Maxwell and the two step Maxwell models.

The comparison between the prediction accuracies (e.g., AARE) of the both modified and two step Maxwell models for predicting different experimentally measured MMMs' permeabilities and the values of their optimized parameters are also reported in Table 5.

As it can be observed in Table 5, employing the two step model to predict MMMs' performance resulted in high AAREs while

after the introduction of β parameter, both permeabilities and selectivities' AAREs were reduced, especially for selectivities. On the other hand, all β parameter values are much smaller than unity (β << 1), which indicates that the estimated permeabilities of gaseous penetrants by the Knudsen flow concept are much higher than their actual values. Also, it should be stated that the l_I optimized values in the two step Maxwell model, which indicate the effective thickness of the formed void volume layer around the filler particles for many MMMs, e.g. Matimid-TiO_2 and ULTEM-FS (TS 610), are smaller than the kinetic diameters of the penetrating molecules. In other words, there is actually no formed void while it is not the case with experimentally measured permeabilities and selectivities that reveal some void formation around the filler particles, as it is also schematically shwn in Figure 5 [39]. Therefore, the optimized value(s) of l_I should be much larger than the kinetic diameter of penetrates. Considering the optimized values of l_I in the modified Maxwell model, they are compatible with the formed voids around the filler particles where the Knudsen flow can be conducted through. In almost all cases of two MMMs in Table 5, the optimized values of l_I and β parameters are in agreement with the known phenomena in the gas penetration.

Table 5
Comparison between the original and modified values of the filler particles loading for different predictive models.

MMM	Gas pairs	ϕ_d	Predictive model					
			The Maxwell		The Bruggeman		The Pal	
			ϕ_d/ϕ_s	ϕ'_d	ϕ_d/ϕ_s	ϕ'_d	ϕ_d/ϕ_s	ϕ'_d
Polysulfone-fumed silica (TS530) [52]	He, N_2	0	0	0	0	0	0	0
		0.05	0.077	0.146	0.054	0.059	0.093	0.124
		0.10	0.154	0.274	0.108	0.117	0.186	0.234
		0.15	0.232	0.389	0.162	0.174	0.279	0.336
		0.20	0.309	0.496	0.216	0.231	0.372	0.431
ULTEM-TS530 (made by melt processing) [54]	CO_2, CH_4	0	0	0	0	0	0	0
		0.01	0.072	0.198	0.01	0.0115	0.068	0.104
		0.07	0.144	0.36	0.073	0.08	0.138	0.199
		0.1	0.217	0.503	0.104	0.114	0.206	0.289

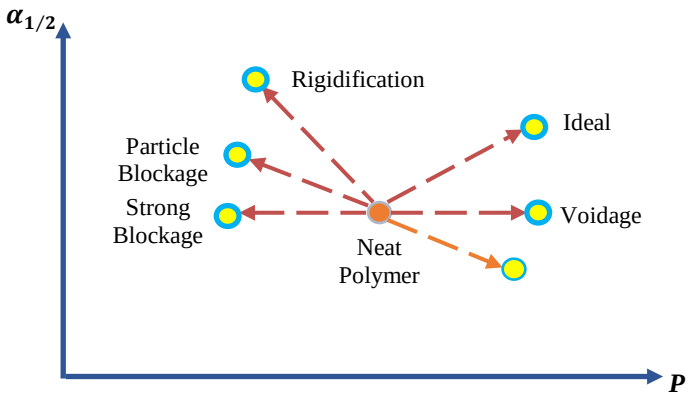

Figure 4. Typical MMMs' morphology diagram and impacts on their separation performance [39].

Some of the original and modified values for filler particles loading are reported in Tables 6 and 7. ϕ_d is the volume fraction of filler particles in MMMs, ϕ_d/ϕ_s is the volume fraction ratio which used in the two step Maxwell model and doesn't consider the swollen MMMs' body after the formation of the voids around the filler particles, and ϕ'_d is the modified volume fraction of the filler particles considering the MMMs as swollen. ϕ'_d values are higher than ϕ_d values so it shows the MMMs are swollen after the void formation around the filler particles.

Table 6
Comparison between the original and modified values of the filler particles loading for the Maxwell model.

MMM	Gas pairs	ϕ_d	ϕ_d/ϕ_s	ϕ'_d
ULTEM-FS (TS610) [54]	He, CH_4	0	0	0
		0.06	0.061	0.095
		0.11	0.112	0.17
		0.18	0.184	0.271
ULTEM-FS (TS720) (made by melt processing) [54]	O_2, N_2	0	0	0
		0.02	0.059	0.072
		0.04	0.117	0.137
		0.10	0.294	0.311
ULTEM-untreated SiO_2 [54]	He, CH_4	0	0	0
		0.04	0.093	0.104
		0.06	0.139	0.153
		0.08	0.186	0.2
		0.10	0.232	0.243
Matrimid-TiO_2 [57]	CO_2, CH_4	0	0	0
		0.05	0.082	0.14
		0.10	0.164	0.262
		0.15	0.247	0.373
		0.20	0.33	0.477
		0.25	0.412	0.575

Table 7
Prediction of different MMMs' permeabilities and selectivities with the formed voids around the filler particles.

MMM	Predictive model	Optimized l_1(Å)	Optimized β	AARE (%)									
				P_{CO_2}	P_{CH_4}	P_{O_2}	P_{N_2}	P_{He}	P_{H_2}	α_{O_2/N_2}	α_{He/CH_4}	α_{He/N_2}	α_{CO_2/CH_4}	α_{H_2/CH_4}
ULTEM-FS (TS610) [54]	TSM[a]	1.6	-		15.68			9.92			15.46			
	TMM[b]	40.2	0.000012		8.65			9.46			13.52			
ULTEM-FS (TS530) (made by solution casting) [54]	TSM	39.3	-		71.64			10			271.98			
	TMM	112.4	0.0000031		22.18			8.75			26.91			

ULTEM-FS (TS720) (made by melt processing) [54]	TSM	124	-			17.22	13.61			22.47					
	TMM	159.6	0.000001			10.65	12.02			10.85					
	TSM	62.6	-		25.13			17.63			50.55				
	TMM	151.4	0.000002		10.15			10.71			7.21				
ULTEM-untreated SiO_2[54]	TSM	32.5	-		6.69			8.04			16.97				
	TMM	40.7	0.000096		4.18			7.49			13.17				
PCPA-FS (TS530) [56]	TSM	33.2	-		38.55			7.14			92.69				
	TMM	66.2	0.000055		14.37			1.09			10.57				
	TSM	34.1	-		36.62				10.72						88.01
	TMM	65.6	0.000066		14.24				3.31						17.55
Matrimid-TiO_2[57]	TSM	2.9	-	4.83	32.08								67.46		
	TMM	7.2	0.0006	3.94	10.37								13.61		
	TSM	1.8	-				31.33	5.38				39.69			
	TMM	9	0.000095				3.16	4.24				7.40			

a: TSM: The two step Maxwell,
b: TMM: The modified Maxwel

5. Conclusions

The knowledge of the MMM's gas separation performance is vital in their structure design for the specified application. Due to some probable defects in MMMs' structure, like the void formation around incorporated filler particles, occurring during their preparation, their separation performance would be changed. Different predictive models were developed to predict the gas separation performance taking into account the probable defects in the MMMs' structure. The current and modified models for the MMMs' separation performance prediction (e.g. two step Maxwell model), especially in case of the void formation around the filler particles, have low prediction accuracies and in some cases are not in agreement with the known phenomena, such as the Knudsen diffusion mechanism. The problem was tried to be solved in the current study by the introduction of β and the modification of the void fraction definition. The current modification resulted in a much higher prediction accuracy for the MMMs with the formed voids around the filler particles and on the other hand, the optimized values of parameters in the current modification of the Maxwell are in agreement with the known phenomena of the gas penetration like the Knudsen flow mechanism.

Nomenclature

T	absolute temperature [K].
l_I	effective thickness of the void (1 Å=10^{-10} m) [Å].
σ_p	Lennard-Jones diameter of filler [Å].
ϕ_m	maximum packing volume fraction of the dispersed phase.
d_{Pore}	pore diameter [Å].
ϕ_I	volume fraction of void space.
P_{MMM}	permeability of mixed matrix membrane (1 Barrer=10^{-10} cm^3 (STP) $cm^{-1}s^{-1}cmHg^{-1}$) [Barrer].
P_C	permeability of polymer as continuous phase [Barrer].
P_d	permeability of filler as dispersed phase [Barrer].
P_I	permeability of void [Barrer].
R	the gas universal constant [cm^3.mol/atm.K].
M_I	the molecular weight of penetrant [g/mol].
ϕ_d	volume fraction of dispersed phase.
ϕ_s	volume fraction of filler in pseudo-two phases.

References

[1] Javaid, A., "Membranes for solubility-based gas separation applications", *Chemical Engineering Journal*, **112** (1-3), 219 (2005).

[2] Basu, S., Cano-Odena, A. and Vankelecom, I. F. J., "Asymmetric matrimid®/[Cu3(BTC)2] mixed-matrix membranes for gas separations", *Journal of Membrane Science*, **362** (1-2), 478 (2010).

[3] Klaassen, R., Feron, P. H. M. and Jansen, A. E., "Membrane contactors in industrial applications", *Chemical Engineering Research and Design*, **83**, 234 (2005).

[4] Nik, O. G., Chen, X. Y. and Kaliaguine, S., "Amine-functionalized zeolite FAU/EMT-polyimide mixed matrix membranes for CO_2/CH_4 separation", *Journal of Membrane Science*, **379** (1-2), 468 (2011).

[5] Nadeali, A., Kalantari, S., Yarmohammadi, M., Omidkhah, M. R., Ebadi Amooghin, A. and Zamani Pedram, M., "CO_2 separation properties of a ternary mixed-matrix membrane using ultraselective synthesized macrocyclic organic compounds", *ACS Sustainable Chemistry & Engineering*, **8** (34), 12775 (2020).

[6] Kalantari, S., Omidkhah, M. R., Ebadi Amooghin, A. and Matsuura, T., "Superior interfacial design in ternary mixed matrix membranes to enhance the CO_2 separation performance", *Applied Materials Today*, **18**, 100491 (2020).

[7] Xin, Q., Shao, W., Ma, Q., Ye, X., Huang, Z., Li, B., Wang, S., Li, H. and Zhang, Y., "Efficient CO_2 separation of multi-permselective mixed matrix membranes with a unique interfacial structure regulated by mesoporous nanosheets", *ACS Applied Materials & Interfaces*, **12** (42), 48067 (2020).

[8] Sarfraz, M. and Ba-Shammakh, M., "ZIF-based water-stable mixed-matrix membranes for effective CO_2 separation from humid flue gas", *The Canadian Journal of Chemical Engineering*, **96** (11), 2475 (2018).

[9] Shariati, A., Omidkhah, M. R. and Zamani Pedram, M., "New permeation models for nanocomposite polymeric membranes filled with nonporous particles", *Chemical Engineering Research and Design*, **90** (4), 563 (2012).

[10] Moore, T. T. and Koros, W. J., "Non-ideal effects in organic-inorganic materials for gas separation membranes", *Journal of Molecular Structure*, **739** (1-3), 87 (2005).

[11] Cong, H., Radosz, M., Towler, B. F. and Shen, Y., "Polymer-inorganic nanocomposite membranes for gas separation", *Separation and Purification Technology*, **55** (3), 281 (2007).

[12] Coulson, J. M., Richardson, J. F. and Sinnott, R. K., Chemical engineering design, Butterworth-Heinemann, Boston, USA, (1996).

[13] Ma, J., Ying, Y., Guo, X., Huang, H., Liu, D. and Zhong, C., "Fabrication of mixed-matrix membrane containing metal-organic framework composite with task-specific ionic liquid for efficient CO_2 separation", *Journal of Materials Chemistry A*, **4** (19), 7281 (2016).

[14] Han, Y. and Ho, W. S. W., "Recent advances in polymeric membranes for CO_2 capture", *Chin. J. Chem. Eng.*, **26** (11), 2238 (2018).

[15] Goh, P. S., Ismail, A. F., Sanip, S. M., Ng, B. C. and Aziz, M., "Recent advances of inorganic fillers in mixed matrix membrane for gas separation", *Separation and Purification Technology*, **81** (3), 243 (2011).

[16] Shimekit, H. M. B. and Maitra, S., "Comparison of predictive models for relative permeability of CO_2 in matrimid-carbon molecular sieve mixed matrix membrane", *Journal of Applied Sciences*, **10**, 1204 (2010).

[17] Ward, J. K. and Koros, W. J., "Crosslinkable mixed matrix membranes with surface modified molecular sieves for natural gas purification: I. Preparation and experimental results", *Journal of Membrane Science*, **377** (1-2), 75 (2011).

[18] Shao, L., Low, B. T., Chung, T. -S. and Greenberg, A. R., "Polymeric membranes for the hydrogen economy: Contemporary approaches and prospects for the future", *Journal of Membrane Science*, **327** (1-2), 18 (2009).

[19] Zhao, H. -Y., Cao, Y. -M., Ding, X. -L., Zhou, M. -Q., Liu, J. -H. and Yuan, Q., "Poly(ethylene oxide) induced cross-linking modification of matrimid membranes for selective separation of CO_2", *Journal of Membrane Science*, **320** (1-2), 179 (2008).

[20] Adewole, J. K., Ahmad, A. L., Ismail, S. and Leo, C. P., "Current challenges in membrane separation of CO_2 from natural gas: A review", *International Journal of Greenhouse Gas Control*, **17** (0), 46 (2013).

[21] Vatanpour, V. and Sanadgol, A., "Surface modification of reverse osmosis membranes by grafting of polyamidoamine dendrimer containing graphene oxide nanosheets for desalination improvement", *Desalination*, **491**, 114442 (2020).

[22] Ye, H., Wang, J., Wang, Y., Chen, X. -P. and Shi, S. -P., "Effects of simultaneous chemical cross-linking and physical filling on separation performances of PU membranes", *IRAN POLYM. J.*, **22** (8), 623 (2013).

[23] Aykac Ozen, H. and Ozturk, B., "Gas separation characteristic of mixed matrix membrane prepared by MOF-5 including different metals", *Sep. Purif. Technol.*, **211**, 514 (2019).

[24] Castarlenas, S., Téllez, C. and Coronas, J., "Gas separation with mixed matrix membranes obtained from MOF UiO-66-graphite oxide hybrids", *J. Membr. Sci.*, **526** (Supplement C), 205 (2017).

[25] Farrokhnia, M., Rashidzadeh, M., Safekordi, A. and Khanbabaei, G., "Fabrication and evaluation of nanocomposite membranes of polyethersulfone/α-alumina for hydrogen separation", *IRAN POLYM. J.*, **24** (3), 171 (2015).

[26] Khdhayyer, M. R., Esposito, E., Fuoco, A., Monteleone, M., Giorno, L., Jansen, J. C., Attfield, M. P. and Budd, P. M., "Mixed matrix membranes based on UiO-66 MOFs in the polymer of intrinsic microporosity PIM-1", *Sep. Purif. Technol.*, **173** (Supplement C), 304 (2017).

[27] Bastani, D., Esmaeili, N. and Asadollahi, M., "Polymeric mixed matrix membranes containing zeolites as a filler for gas separation applications: A review", *Journal of Industrial and Engineering Chemistry*, **19** (2), 375 (2013).

[28] Bakhtiari, O. and Sadeghi, N., "Mixed matrix membranes' gas separation performance prediction using an

analytical model", *Chemical Engineering Research and Design*, **93**, 710 (2015).

[29] Etemadi, H., Yegani, R., Seyfollahi, M. and Rabiee, M., "Synthesis, characterization, and anti-fouling properties of cellulose acetate/polyethylene glycol-grafted nanodiamond nanocomposite membranes for humic acid removal from contaminated water", *IRAN POLYM. J.*, **27** (6), 381 (2018).

[30] Liang, C. -Y., Uchytil, P., Petrychkovych, R., Lai, Y. -C., Friess, K., Sipek, M., Mohan Reddy, M. and Suen, S. -Y., "A comparison on gas separation between PES (polyethersulfone)/MMT (Na-montmorillonite) and PES/TiO_2 mixed matrix membranes", *Separation and Purification Technology*, **92** (0), 57 (2012).

[31] Pirouzfar, V. and Omidkhah, M. R., "Mathematical modeling and optimization of gas transport through carbon molecular sieve membrane and determining the model parameters using genetic algorithm", *IRAN POLYM. J.*, **25** (3), 203 (2016).

[32] Karatay, E., Kalıpçılar, H. and Yılmaz, L., "Preparation and performance assessment of binary and ternary PES-SAPO 34-HMA based gas separation membranes", *Journal of Membrane Science*, **364** (1-2), 75 (2010).

[33] Shimekit, B., Mukhtar, H. and Murugesan, T., "Prediction of the relative permeability of gases in mixed matrix membranes", *Journal of Membrane Science*, **373** (1-2), 152 (2011).

[34] Pal, R., "Permeation models for mixed matrix membranes", *Journal of Colloid and Interface Science*, **317** (1), 191 (2008).

[35] Feng, S., Bu, M., Pang, J., Fan, W., Fan, L., Zhao, H., Yang, G., Guo, H., Kong, G., Sun, H., Kang, Z. and Sun, D., "Hydrothermal stable ZIF-67 nanosheets via morphology regulation strategy to construct mixed-matrix membrane for gas separation", *Journal of Membrane Science*, **593**, 117404 (2020).

[36] Petsi, A. J. and Burganos, V. N., "Interphase layer effects on transportin mixed matrix membranes", *Journal of Membrane Science*, **421-422**, 247 (2012).

[37] Chehrazi, E., Raef, M., Noroozi, M. and Panahi-Sarmad, M., "A theoretical model for the gas permeation prediction of nanotube-mixed matrix membranes: Unveiling the effect of interfacial layer", *J. Membr. Sci.*, **570-571**, 168 (2019).

[38] Monsalve-Bravo, G. M., Smart, S. and Bhatia, S. K., "Simulation of multicomponent gas transport through mixed-matrix membranes", *J. Membr. Sci.*, **577**, 219 (2019).

[39] Hashemifard, S. A., Ismail, A. F. and Matsuura, T., "Prediction of gas permeability in mixed matrix membranes using theoretical models", *Journal of Membrane Science*, **347** (1-2), 53 (2010).

[40] Hashemifard, S. A., Ismail, A. F. and Matsuura, T., "A new theoretical gas permeability model using resistance modeling for mixed matrix membrane systems", *Journal of Membrane Science*, **350** (1-2), 259 (2010).

[41] Vu, D. Q., Koros, W. J. and Miller, S. J., "Mixed matrix membranes using carbon molecular sieves: II. Modeling permeation behavior", *Journal of*

Membrane Science, **211** (2), 335 (2003).

[42] Mohammad Gheimasi, K., Mohammadi, T. and Bakhtiari, O., "Modification of ideal MMMs permeation prediction models: Effects of partial pore blockage and polymer chain rigidification", *Journal of Membrane Science*, **427**, 399 (2013).

[43] Nasir, R., Mukhtar, H. and Man, Z., "Prediction of gas transport across amine mixed matrix membranes with ideal morphologies based on the Maxwell model", *RSC Advances*, **6** (36), 30130 (2016).

[44] Yang, W. Y., Cao, W., Chung, T. -S. and Morris, J., Applied numerical methods using Matlab, John Wiley & Sons Inc., (2005).

[45] Lee, E. -S. and Youn, S. -K., "Finite element analysis of wrinkling membrane structures with large deformations", *Finite Elem. Anal. Des.*, **42** (8), 780 (2006).

[46] Aroon, M. A., Ismail, A. F., Matsuura, T. and Montazer-Rahmati, M. M., "Performance studies of mixed matrix membranes for gas separation: A review", *Separation and Purification Technology*, **75** (3), 229 (2010).

[47] Erucar, I. and Keskin, S., "Computational screening of metal organic frameworks for mixed matrix membrane applications", *Journal of Membrane Science*, **407-408** (0), 221 (2012).

[48] Mahajan, R. and Koros,W. J., "Mixed matrix membrane materials with glassy polymers, Part 1", *Polymer Engineering and Science*, **42**, (2002).

[49] Chung, T. -S., Jiang, L. Y., Li, Y. and Kulprathipanja, S., "Mixed matrix membranes (MMMs) comprising organic polymers with dispersed inorganic fillers for gas separation", *Progress in Polymer Science*, **32** (4), 483 (2007).

[50] Hosseini, S. S., Li, Y., Chung, T. -S. and Liu, Y., "Enhanced gas separation performance of nanocomposite membranes using MgO nanoparticles", *J. Membr. Sci.*, **302** (1-2), 207 (2007).

[51] Shelekhin, A. B., Dixon, A. G. and Ma, Y. H., "Adsorption, permeation, and diffusion of gases in microporous membranes. II. Permeation of gases in microporous glass membranes", *Journal of Membrane Science*, **75** (3), 233 (1992).

[52] Ahn, J., Chung, W. -J., Pinnau, I. and Guiver, M. D., "Polysulfone/silica nanoparticle mixed-matrix membranes for gas separation", *Journal of Membrane Science*, **314** (1-2), 123 (2008).

[53] Baker, R. W., Membrane technology and applications, Second ed., John Wiley & Sons Inc., (2004).

[54] Takahashi, S. and Paul, D. R., "Gas permeation in poly(ether imide) nanocomposite membranes based on surface-treated silica. Part 1: Without chemical coupling to matrix", *Polymer*, **47** (21), 7519 (2006).

[55] Bakhtiari, O. and Sadeghi, N., "The formed voids around the filler particles impact on the mixed matrix membranes' gas permeabilities", *International Journal of Chemical Engineering and Applications*, **5** (2), 198 (2014).

[56] Kono, T., Hu, Y., Masuda, T., Tanaka, K., Priestley, R. D. and Freeman, B. D., "Effect of fumed silica nanoparticles on the gas permeation properties of substituted polyacetylene membranes", *Polymer Bulletin*, **58**, 995 (2007).

[57] Moghadam, F., Omidkhah, M. R., Vasheghani-Farahani, E., Zamani Pedram, M. and Dorosti, F., "The effect of TiO_2 nanoparticles on gas transport properties of Matrimid5218-based mixed matrix membranes", *Separation and Purification Technology*, **77** (1), 128 (2011).